# RILEM TC 247-DTA round robin test
## carbonation and chloride penetration testing of alkali-activated concretes

Gluth, Gregor J.G.; Arbi, Kamel; Bernal, Susan A.; Bondar, Dali; Castel, Arnaud; Chithiraputhiran, Sundararaman; Dehghan, Alireza; Dombrowski-Daube, Katja; Dubey, Ashish; Ducman, Vilma

**DOI**
10.1617/s11527-020-1449-3

**Publication date**
2020

**Document Version**
Final published version

**Published in**
Materials and Structures/Materiaux et Constructions

Materials and Structures (2020) 53:21
https://doi.org/10.1617/s11527-020-1449-3

ORIGINAL ARTICLE

# RILEM TC 247-DTA round robin test: carbonation and chloride penetration testing of alkali-activated concretes

**Gregor J. G. Gluth · Kamel Arbi · Susan A. Bernal · Dali Bondar · Arnaud Castel · Sundararaman Chithiraputhiran · Alireza Dehghan · Katja Dombrowski-Daube · Ashish Dubey · Vilma Ducman · Karl Peterson · Penny Pipilikaki · Siska L. A. Valcke · Guang Ye · Yibing Zuo · John L. Provis**

Received: 26 November 2019 / Accepted: 4 February 2020


**Abstract** Many standardised durability testing methods have been developed for Portland cement-based concretes, but require validation to determine whether they are also applicable to alkali-activated materials. To address this question, RILEM TC 247-DTA 'Durability Testing of Alkali-Activated Materials' carried out round robin testing of carbonation and chloride penetration test methods, applied to five different alkali-activated concretes based on fly ash, blast furnace slag or metakaolin. The methods appeared overall to demonstrate an intrinsic precision comparable to their precision when applied to conventional concretes. The ranking of test outcomes for pairs of concretes of similar binder chemistry was satisfactory, but rankings were not always reliable when comparing alkali-activated concretes based on

This article was prepared within the framework of RILEM TC 247-DTA. The article has been reviewed and approved by all members of the TC.

*TC Membership*:

*Chair*: John L. Provis, UK.

*Deputy Chair*: Frank Winnefeld, Switzerland.

*TC Members*: Kamel Arbi, Netherlands; P.A. Muhammad Basheer, UK; Susan A. Bernal, UK; Dali Bondar, UK; Lorenza Carabba, Italy; Arnaud Castel, Australia; Maria Chiara Bignozzi, Italy; Anja Buchwald, Netherlands; Huisu Chen, P.R. China; Sundaraman Chithiraputhiran, USA; Francesco Colangelo, Italy; Andrzej Cwirzen, Sweden; Martin Cyr, France; Alireza Dehghan, Canada; Katja Dombrowski-Daube, Germany; Ashish Dubey, USA; Vilma Ducman, Slovenia; Ana Fernández-Jiménez, Spain; Ellis M. Gartner, France; Gregor J.G. Gluth, Germany; R. Douglas Hooton, Canada; Kazuo Ichimiya, Japan; Elie Kamseu, Cameroon; Lesley S.-C. Ko, USA; Sabina Kramar, Slovenia; Pavlo V. Kryvenko, Ukraine; Yuwei Ma, P.R. China; Isabel Martins, Portugal; Sreejith V. Nanukuttan, UK; Angel Palomo, Spain; Karl Peterson, Canada; Penny Pipilikaki, Netherlands; Francisca Puertas, Spain; Aljoša Šajna, Slovenia; Jay G. Sanjayan, Australia; Caijun Shi, P.R. China; Marios N. Soutsos, UK; Dietmar Stephan, Germany; Arezki Tagnit-Hamou, Canada; Monique Tognonvi, Canada; Manuel Torres, Spain; Siska L.A. Valcke, Netherlands; Arie van Riessen, Australia; Jannie S.J. van Deventer, Australia; Jeanette H.M. Visser, Netherlands; Steffen Wache, Germany; Claire E. White, USA; Guang Ye, Netherlands; Yibing Zuo, Netherlands.

**Electronic supplementary material** The online version of this article (https://doi.org/10.1617/s11527-020-1449-3) contains supplementary material, which is available to authorized users.

G. J. G. Gluth
Bundesanstalt für Materialforschung und -prüfung (BAM), Unter den Eichen 87, 12205 Berlin, Germany

K. Arbi · G. Ye · Y. Zuo
Faculty of Civil Engineering and Geosciences, Delft University of Technology, Stevinweg 1, 2628 CN Delft, The Netherlands

K. Arbi
Delta Concrete Consult B. V., Marconiweg 2, 4131 PD Vianen, The Netherlands

Published online: 13 February 2020

different precursors. Accelerated carbonation testing gave similar results for fly ash-based and blast furnace slag-based alkali-activated concretes, whereas natural carbonation testing did not. Carbonation of concrete specimens was observed to have occurred already during curing, which has implications for extrapolation of carbonation testing results to longer service life periods. Accelerated chloride penetration testing according to NT BUILD 443 ranked the tested concretes consistently, while this was not the case for the rapid chloride migration test. Both of these chloride penetration testing methods exhibited comparatively low precision when applied to blast furnace slag-based concretes which are more resistant to chloride ingress than the other materials tested.

**Keywords** Alkali-activated concrete · Blast furnace slag · Fly ash · Metakaolin · Carbonation · Chloride penetration · Durability testing · Round robin

## 1 Introduction

Although alkali-activated slag concretes (a subset of alkali-activated concretes) have proven to be sufficiently durable for use in real-world applications [1–3], the long-term durability of other alkali-activated concretes and reinforced structures made from them is still an open issue, and many factors that influence alkali-activated materials (AAMs) in general are not fully understood [4]. The uncertainties that remain in this regard are partly due to the fact that alkali-activated materials comprise a wide range of chemical compositions, which can yield very different microstructural characteristics and also lead to prominence of different degradation mechanisms within this broad class of materials.

A major aspect of the durability of reinforced concrete structures is the protection that the concrete provides to the embedded steel reinforcement. The two most important deterioration mechanisms in this regard are depassivation of the steel by ingress of $CO_2$ with associated decrease of the pH of the pore solution of the concrete (carbonation), and localised depassivation of the steel caused by chloride ions that reach the steel–concrete interface (chloride penetration) [5–7]. For alkali-activated concretes, as for conventional Portland cement-based concretes, the time to onset of reinforcement corrosion is determined by the conditions (e.g. pH, redox conditions, chloride concentration) at the steel–concrete interface [8, 9], and the rates of carbonation and chloride penetration. A considerable number of studies have been conducted concerning the rates of carbonation and chloride penetration in alkali-activated concretes and mortars, for example [1, 2, 10–23], but the data currently available do not yet lead to a comprehensive description of the transport and influence of $CO_2$ and chloride in these materials.

S. A. Bernal
School of Civil Engineering, The University of Leeds, Leeds LS2 9JT, UK

S. A. Bernal · J. L. Provis (✉)
Department of Materials Science and Engineering, University of Sheffield, Sheffield S1 3JD, UK
e-mail: j.provis@sheffield.ac.uk

D. Bondar
School of Natural and Built Environment, Queen's University Belfast, Belfast BT9 5AG, UK

A. Castel
School of Civil and Environmental Engineering, University of Technology Sydney, Ultimo, NSW 2007, Australia

S. Chithiraputhiran · A. Dubey
Corporation Innovation Center, USG Corporation, 700 North Highway 45, Libertyville, IL 60048, USA

A. Dehghan · K. Peterson
Department of Civil and Mineral Engineering, University of Toronto, 35 St. George Street, Toronto, ON M5S 1A4, Canada

K. Dombrowski-Daube
Institut für Bergbau und Spezialtiefbau, Technische Universität Bergakademie Freiberg, Gustav-Zeuner-Straße 1A, 09599 Freiberg, Germany

V. Ducman
Slovenian National Building and Civil Engineering Institute (ZAG), Dimičeva 12, 1000 Ljubljana, Slovenia

P. Pipilikaki · S. L. A. Valcke
Structural Reliability, Netherlands Organisation for Applied Scientific Research (TNO), Stieltjesweg 1, 2628 CK Delft, The Netherlands

To quantify the capability of alkali-activated concrete to protect embedded steel reinforcement from the ingress of aggressive agents that may lead to its depassivation, reliable and meaningful test methods for carbonation and chloride ingress are required. Availability of such methods is essential to performance-based standardisation, and would also facilitate scientific progress by making results obtained in different laboratories comparable with each other. Such test methods would be a means to assess the relative benefits and limitations of specific alkali-activated concrete mix-designs in applications for reinforced structures. However, all widely used carbonation and chloride penetration test methods were originally developed for, and adjusted to, conventional concretes. Because of the significant compositional and microstructural differences between concretes based on conventional (Portland and blended) cements and those containing alkali-activated cements, it is unclear whether, or to what extent, these methods can also yield meaningful and precise results for alkali-activated materials.

To address these issues, RILEM TC 247-DTA carried out a round robin testing programme on various carbonation and chloride penetration test methods, assessing five alkali-activated concretes based on fly ash, blast furnace slag or metakaolin. The selected tests are established methods in the field of concrete technology, described in pertinent EN, NordTest and ASTM standards. A total of 10 laboratories from Europe, North America, and Australasia participated in the testing. The present report describes the results obtained, and discusses some of their implications.

## 2 Materials and methods

### 2.1 Starting materials, concrete mix-designs and curing

The solid binder materials for the concretes were hard coal fly ash (FA), supplied by BauMineral (Germany); blast furnace slag (BFS), supplied by ECOCEM® (France); and flash-calcined metakaolin (MK), supplied by Argeco (France). The activator solutions were generally made from sodium silicate solution, adjusted to the targeted compositions by adding appropriate amounts of water and sodium hydroxide. The aggregates used in each laboratory were usually sourced from local suppliers, thus, their compositions and the details of the grading curves differed between laboratories. More detailed characterisation of these materials, and of the binders and concretes designed from them, is reported in the first published paper resulting from the work of this TC [24].

Two BFS-based concretes, two fly ash-based concretes, and one metakaolin-based concrete were produced and tested, with one concrete designed to exhibit a 'moderate' performance and the other concrete designed to exhibit a 'high' performance, respectively [24]. In this paper, the concretes based on different binder materials (fly ash, BFS, or metakaolin) will be referred to as different 'classes' of alkali-activated concretes. The mix designs, together with the targeted compressive 28-day strengths ('design strengths'), of the concretes are shown in Table 1, and a more detailed discussion of these mixes and the rationale behind their design is provided in [24].

Concretes were cured before testing as follows: 2 days (or until demouldable) in covered or sealed moulds at 20–23 °C, and subsequently to 28 days of age in tightly closed plastic bags at 20–23 °C. For the natural carbonation testing and the rapid chloride permeability tests, some laboratories applied differing curing times, as described in Sects. 2.3 and 2.6.

### 2.2 Accelerated carbonation testing

Accelerated carbonation testing was performed according to EN 13295:2004 [25]. Generally, concrete prisms with dimensions of at least 100 mm × 100 mm × 500 mm were used; one laboratory (referred to as laboratory *H*) employed cubic samples with an edge length of 50 mm. After curing as described in Sect. 2.1, specimens were dry conditioned at (21 ± 2) °C/(60 ± 10) % relative humidity (RH) until their weight change was less than 0.2% in a 24-h period, but at least for 14 days. Subsequently, the specimens were transferred to a carbonation cabinet in which an atmosphere with a $CO_2$ concentration of 1 vol% and a RH of (60 ± 10) % was maintained. After specified periods of exposure to $CO_2$, specimens were removed from the cabinet and their depths of carbonation determined by spraying phenolphthalein indicator solution onto freshly broken surfaces of the specimens. Visual observation of colour change boundaries results in the need for human judgement

**Table 1** Mix designs (kg/m$^3$) and approximate design strengths of the alkali-activated concretes

| Concrete | Precursor (kg/m$^3$) | Sodium silicate dose[a] | Sodium hydroxide dose[b] | Water/binder mass ratio[c] | Aggregate grading[d] | Design air content (%)[e] | Design density (kg/m$^3$)[e] | Design strength (MPa) |
|---|---|---|---|---|---|---|---|---|
| S3a | BFS, 375 | 2.69 | 4 | 0.382 | 40% sand 0–4 mm, 60% gravel 4–16 mm, to meet A/B 16 curve | 1.0 | 2375 | 60 |
| S1b | BFS, 357 | 1.34 | 3 | 0.420 | 40% sand 0–4 mm, 60% gravel 4–16 mm, to meet A/B 16 curve | 1.0 | 2364 | 35 |
| FA2 | FA, 425 | 16.5 | 5.9 | 0.223 | To meet A/B 16 curve | 3.0 | 2350 | 65 |
| FA8 | FA, 425 | 16.5 | 5.9 | 0.253 | To meet A 16 curve | 3.0 | 2324 | 50 |
| MK1 | MK, 350 | 32.3 | 2.7 | 0.393 | To meet A/B 16 curve | 1.0 | 2186 | 60 |

[a]Represented as g $Na_2Si_2O_5$/100 g precursor, where the solid component of sodium silicate solution of modulus 2.0 is given as $Na_2Si_2O_5$. Where a different modulus of sodium silicate solution was used in some labs, the total activator dose was held constant but the division between silicate and hydroxide constituents was changed

[b]Represented as g NaOH/100 g precursor

[c]Including water added within the aqueous activator solution, or separately from the activator, and with "binder" defined as the sum of precursor and solid activator components

[d]Participants were instructed to match the A 16 (coarse) or A/B 16 (between coarse A and fine B) curves of DIN 1045-2 as closely as possible; some labs could only access all-in aggregates or only two different aggregate fractions and this gave some intrinsic variability, whereas others were able to blend multiple fractions to give a closer match to the specified curve

[e]The air content and density given here are nominal values used in mix design, and will vary depending on the nature of the aggregates, mixing and casting protocols used in each lab

to be applied; each laboratory applied its established processes and expertise in defining exactly how faint the pink indicator colouration would be at the point defined as the carbonated-uncarbonated boundary. EN 13295 specifies an exposure time of 56 days to determine the depth of carbonation, $d_k$ [25], but additional time points were used here to provide deeper insight into the carbonation process. Several laboratories reported that—deviating from EN 13295, which prescribes that the depth of carbonation be measured 60 ($\pm$ 5) min after spraying the phenolphthalein solution [25]—they took the readings of the depths of carbonation within $\sim$ 15 min after spraying the phenolphthalein solution, because after longer times the colour of the solution on the broken surfaces became faint. It did not appear that the difference between reading at 15 and 60 min (in cases where the latter was possible) gave a significant difference in the results.

### 2.3 Natural carbonation testing

A procedure to test the relative carbonation resistance of concretes under natural conditions or under conditions approximating natural exposure is described in CEN/TS 12390-10: 2007 [26], and was adopted in this study, but with tests initiated at 28 days of curing instead of selecting an exposure time by strength comparison with reference concretes. However, one laboratory (referred to as laboratory *G*) applied different curing times to approximate the procedure prescribed in CEN/TS 12390-10 [26]. In this laboratory the curing times (sealed) before exposure to $CO_2$ were: S1b: 3 days, S3a: 2 days, FA2: 13 days, FA8: 13 days, MK1: 1 day.

For natural carbonation testing, concrete prisms with dimensions of at least 100 mm $\times$ 100 mm $\times$ 400 mm were used, as prescribed in CEN/TS 12390-10 [26]. In accordance with the standard, the depths of carbonation were determined after specified exposure times by spraying phenolphthalein indicator solution on freshly broken surfaces of the concrete specimens. As with the accelerated carbonation testing

described in Sect. 2.2, several laboratories reported that readings had to be taken within time periods significantly less than 60 min after spraying the solution.

Exposure to $CO_2$ was started immediately after curing without any specimen pre-conditioning, either under controlled exposure conditions using natural levels of $CO_2$ ('indoor'), under natural conditions protected from rainfall ('sheltered'), or under natural conditions exposed to rainfall ('exposed'). The 'indoor' exposure conditions differed moderately between laboratories, the temperature generally being (20 ± 5) °C and the RH ranging between 50 and 65% (one laboratory reported RH ≥ 50%). One participant conducted carbonation of samples in an office; the temperature during that exposure was recorded to be in the range 19–27 °C and the RH in the range 25–58% (see footnotes to Table S3).

### 2.4 Accelerated chloride penetration test

Accelerated chloride penetration testing was performed according to NordTest NT BUILD 443 [27]. In summary, the test consists of assessing three concrete cylinders with a diameter of at least 75 mm, saturated with $Ca(OH)_2$ solution and coated except for one face to allow unidimensional chloride ingress, by immersing them in 165 g/L NaCl solution at (23 ± 2) °C. After a minimum exposure time of 35 days, chloride ingress is analysed by profile grinding of the specimens.[1] The effective chloride transport coefficient, $D_e$, is then computed by fitting the measured chloride profile to the pertinent equation in the standard, derived from Fick's second law of diffusion [28].

### 2.5 Rapid chloride migration (RCM) test

Chloride migration coefficients of the alkali-activated concretes were determined according to the procedure described in NT BUILD 492 [29], often referred to as the rapid chloride migration (RCM) test. The test is applied to triplicate concrete slices ($\varphi$ 100 mm × 50 mm), which are vacuum saturated in $Ca(OH)_2$ solution then mounted in a test cell. Therein, one face of each specimen is immersed in 10% NaCl solution, and the other in 0.3 M NaOH solution. A voltage of 10–60 V is applied between the two faces for 6–96 h, where the voltage used in each test is selected from a look-up table in the standard depending on the initial conductivity of the specimens. After this period, the chloride penetration depth is determined by spraying a 0.1 M $AgNO_3$ solution onto the axially split surfaces of the specimens. The non-steady-state chloride migration coefficient, $D_{nssm}$, is computed from the observed penetration depth using the pertinent formula in the standard, obtained from the Nernst-Planck equation [30], and assuming a $Cl^-$ concentration of 0.07 M at the colour-change (white-colourless) boundary. The validity of this assumption for alkali-activated materials has been questioned in the past [31], but it was adopted here in the absence of a standardised method that includes this effect explicitly.

### 2.6 Rapid chloride permeability test (RCPT)

Another method that is widely used to assess the chloride penetration resistance of concretes is the test described in ASTM C1202 [32],[2] which is a measurement of the electrical conductivity of concrete. This test is often referred to as the rapid chloride permeability test (RCPT).

To conduct the test, concrete slices with a thickness of 50 mm and preferably with a diameter of 95–100 mm are vacuum-saturated, and mounted in a dedicated set-up described in ASTM C1202. A voltage of 60 V is then applied between the two end faces of the specimens for 6 h at a laboratory temperature of 20–25 °C, while recording the current at regular intervals. The total charge, $Q$, passed over that period is computed and reported as the test result.

In the present testing programme, three laboratories performed the RCPT according to ASTM C1202 on specimens cured for 28 days under the conditions described in Sect. 2.1, while two of these laboratories additionally tested specimens cured under the same conditions for 56 or 90 days.

[1] One laboratory (referred to as laboratory *B*) performed exposure to NaCl according to NT BUILD 443, but instead of profile grinding, determined a chloride ingress depth using the $AgNO_3$ spray method as in NT BUILD 492 (see Sect. 2.5), assuming a $Cl^-$ concentration at the colour-change boundary of 0.10 M, and used this to compute the chloride transport coefficients.

[2] The testing programme was initiated in 2012, and therefore the corresponding release of ASTM C1202 was applied in the majority of participating laboratories.

## 3 Reporting of results

The participating laboratories reported their results in preformatted templates for each test; in some cases, explanatory notes were submitted in addition to the completed templates. The reported deviations from standard procedures are described in Sect. 2. Six laboratories reported accelerated carbonation data; five laboratories reported natural carbonation data; and seven laboratories reported chloride penetration data. All results are given, summarised as the laboratories' mean values with their standard deviations, in the Electronic Supplementary Material (Tables S1–S8) accompanying this article. In Sect. 4, these results are graphically presented and discussed.

## 4 Results and discussion

### 4.1 Accelerated carbonation testing

Figure 1 shows the results of the accelerated carbonation testing of the fly ash-based concretes and the BFS-based concretes. In all cases where a laboratory had tested both the moderate-performance (FA8 and S1b) and the higher-performance (FA2 and S3a) concretes, the results were ranked in the expected order, i.e. the high-performance concrete produced using each precursor exhibited considerably lower depths of carbonation than its moderate-performance counterpart. The gas permeability of concrete FA8 was measured to be greater by a factor of $\sim$ 3 than that of FA2 after a curing time of 28 days [33], confirming that lower performance in durability testing involving transport phenomena can be expected from FA8.

As an estimate of the reproducibility of the method, the standard deviation (sd) and the coefficient of variation (COV) of the mean results reported by the different laboratories was calculated. For the depth of carbonation of the fly ash-based concretes after 56 days of carbonation (the exposure duration before determination of the depth of carbonation, specified in EN 13295 [25]), these values were sd = 5.9–7.4 mm, and COV = 40.6–45.4%; for the BFS-based concretes these values were sd = 2.2–3.3 mm, and COV = 14.2–33.5% (Table S9). These values may be compared with those given in the standard and in the literature: EN 13295 [25] gives sd = $0.21 \times d_k + 0.64$ (in mm), where $d_k$ is the average carbonation depth, as the reproducibility of the method when different laboratories test the same material. This results in an expected range of sd = 3.4–4.5 mm for the fly ash-based concretes, and 2.7–3.9 mm for the BFS-based concretes. In a variability study of the carbonation depths of different batches of concretes based on three different Portland-blended cements [34], it was found that the resulting COVs (obtained in two laboratories) were between 12 and 37%, so the results presented here for AAMs are well aligned with the reproducibility of that analysis of conventional concretes. Some laboratories reported the observation of a rather diffuse colour change front for fly ash-based AAM concretes in this testing programme, which may have influenced the greater sd and COV for those concretes.

In the present round robin, the scatter of the data obtained includes some variability of the properties of concrete produced in different laboratories [24], as well as the between-laboratory variability inherent to the test method. Therefore, these comparisons suggest that the method described in EN 13295 [25] is sufficiently precise to correctly rank alkali-activated concretes of similar chemistry according to their respective carbonation resistances. However, comparison with natural carbonation results (presented in the following section) is necessary to assess whether the test is truly representative of field performance.

### 4.2 Natural carbonation testing: indoor

The results of the carbonation testing under natural levels of $CO_2$ exhibit considerable differences between the alkali-activated concretes based on the different precursors used here (Fig. 2). The concretes based on low-Ca binders (fly ash, metakaolin) generally exhibited substantially larger depths of carbonation than the BFS-based concretes. Within the class of low-Ca binder concretes, the fly ash-based concretes appear to perform better than the metakaolin-based concretes, though the scatter of the fly ash results is considerable and may again be related to difficulties in identifying the precise carbonation front location which were noted by some participating laboratories. This is consistent with expectations based on the water contents of the alkali-activated concretes based on fly ash and on metakaolin; the metakaolin-based concrete had a much higher water/binder ratio (0.393,

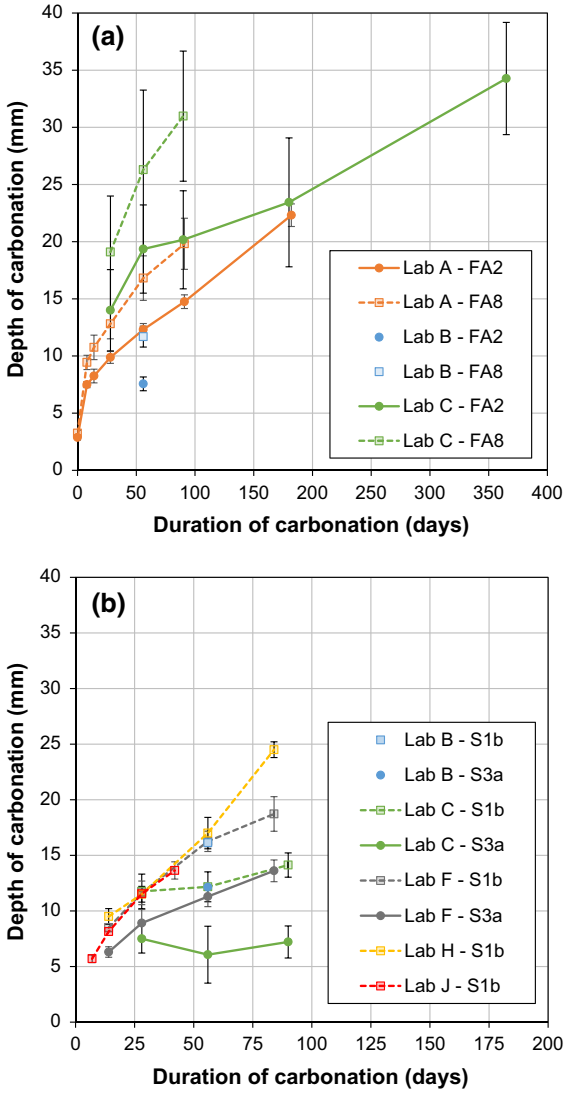


**Fig. 1** Results of accelerated carbonation testing according to EN 13295 (1% $CO_2$, [25]) of **a** the fly ash-based concretes FA2 and FA8, and **b** the BFS-based concretes S1b and S3a. Note the different ranges of the abscissae in panels **a** and **b**. *Error bars* represent one standard deviation in each direction from the mean, within the replicate results reported by each laboratory

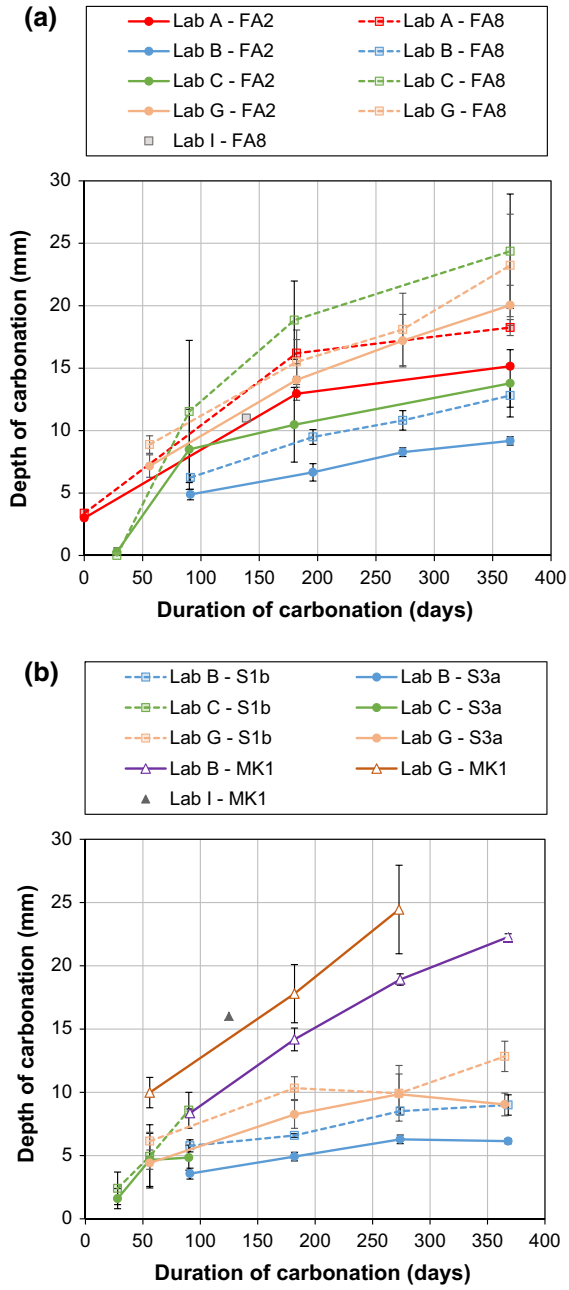


**Fig. 2** Results of carbonation testing under conditions approximating natural exposure ('indoor'), for (**a**) the fly ash-based concretes FA2 and FA8, and (**b**) the BFS-based concretes S1b and S3a, and the metakaolin-based concrete MK1. *Error bars* represent one standard deviation in each direction from the mean, within the results recorded by each laboratory

compared to 0.223 for FA2 and 0.253 for FA8). The BFS-based concretes do have water/binder ratios comparable to that of the metakaolin-based concrete (0.382 and 0.420 for S3a and S1b, respectively). Nevertheless, the higher content of calcium content, which is able to absorb $CO_2$ as it carbonates, and also contributes to microstructural refinement of the slag-based binder [35] gives a significantly reduced carbonation rate for the BFS-based AAM concretes.

The evident performance differences between the fly ash-based concretes and the BFS-based concretes under natural conditions (Fig. 2) were much less

pronounced in accelerated carbonation testing (Fig. 1). For example, in laboratory *B*, the slag-based concretes exhibited a higher depth of carbonation than the fly ash-based concretes after 56 days of accelerated exposure, which is the reverse of the observations under natural conditions. This discrepancy between accelerated and natural carbonation testing can be assigned to the peculiarities of the pore solution compositions of alkali-activated concretes. It has been shown, by modelling as well as experimentally [36–38] that because the pore solutions of alkali-activated concretes are usually dominated by sodium ions, the $CO_2$ concentration of the exposure atmosphere strongly influences the carbonate/bicarbonate equilibrium in the pore solution, driving that equilibrium toward dominance by bicarbonate at higher $CO_2$ concentrations [39]. This, in turn, controls the pH of the pore solution. Buffering by the carbonate-bicarbonate deprotonation equilibrium maintains the pH at around 11 under natural carbonation conditions, as compared to around 9 at elevated $p_{CO2}$. Such effects are not seen in Portland cement as its carbonation process is dominated by calcium carbonate formation, without such strong influence from soluble alkali carbonates.

Thus, an increase in $CO_2$ concentration from 0.03–0.04% (natural carbonation) to 1% (conditions of EN 13295) not only induces a significant decrease in the pH of the carbonated pore solution in an alkali-activated material, but also changes the nature of the precipitated carbonation products [36–38]. This can influence the outcomes of carbonation testing. Additional complications may arise from the fact that at a $CO_2$ concentration of 1%, the pH of the carbonated pore solution is within the colour-change transition range of the phenolphthalein indicator [38], and so any colour change boundary may become difficult to observe visually, or may appear as a large faint-pink "partially carbonated" zone. This can lead to difficulties in performing the carbonation depth readings, and/or cause systematic bias between readings taken on AAM concretes with low-Ca binders and those with high-Ca binders.

In natural carbonation as well as in accelerated carbonation testing, concretes with the same precursor that had been designed for different performance levels, nearly always exhibited results in the expected order. With only one exception (S3a tested in laboratory *G* at 273 days), the depths of carbonation of the concrete designed for moderate performance concrete were consistently higher than those of the corresponding high-performance concrete (Fig. 2). However, the absolute differences between the values for corresponding high- and moderate-performing concretes tended to be lower under indoor-natural carbonation testing than in accelerated carbonation testing, even though the natural carbonation exposure durations were much longer. The increased $CO_2$ concentration used in accelerated testing can be expected to exaggerate any differences in performance of concretes of similar chemistry. Comparing the results of the accelerated carbonation testing with the results of the natural carbonation testing in this study indicates that only natural carbonation is expected to give a true indication of field performance when comparing between binders of fundamentally different chemistry.

The sd and COVs of the mean depths of indoor-natural carbonation after an exposure duration of 365(± 3) days were 4.5–5.3 mm and 26.9–30.8% for the fly ash-based concretes, and 2.1–2.7 mm and 24.9–27.1% for the BFS-based concretes, respectively (Table S10). Thus, compared to the accelerated carbonation testing, these values were lower (indicating less scatter under indoor-natural conditions) for the fly ash-based concretes, and similar for the BFS-based concretes. This improvement was seen even though the variability of the data in this case also includes the variability of the exposure conditions (temperature and RH) in the different laboratories as well as the deviating curing conditions in one laboratory (Sect. 2.3).

The RH imposed during carbonation testing has a greater influence on the saturation level of the concrete, and consequently the carbonation rate of cementitious materials with a fine pore structure, compared to cementitious materials with a coarser pore structure [40, 41]. As alkali-activated BFS generally has a finer pore structure than alkali-activated fly ashes [35], it can be expected that the influence of the variation of the exposure conditions on the results was more pronounced for the BFS-based concretes. These observations suggest that indoor-natural carbonation testing will be of significantly better precision than accelerated carbonation testing to compare the performance of alkali-activated concretes of different strength classes, if the natural carbonation testing is conducted under identical temperature/RH conditions and using specimens cured under identical

conditions. This also brings the advantage that the test conditions are much less divergent from expected service conditions, but comes at the cost of a longer test duration. This finding differs from published results for Portland cement and blended-Portland concretes [42], where a very strong correlation between accelerated (4% $CO_2$) and indoor-natural carbonation conditions was observed across a wide range of concretes, and without any effective difference in ranking of various concretes under 1, 4 or 10% $CO_2$ levels.

Since the method described in CEN/TS 12390-10 [26] is a comparative method, the standard document itself does not give information on the expected reproducibility, with which the above values could be compared. However, a detailed analysis of results obtained through an inter-laboratory study using an earlier draft of that testing method identified a COV of 30% for Portland cement concretes made from the same cement and mix design but with different locally available aggregates in each laboratory [43], and the COV values obtained here are very consistent with those findings. The use of identical aggregates and centrally-prepared concretes shipped to all laboratories in a second round of testing in [43] was found to give a reduction in COV to around 12%, but such an approach was not practical within the constraints of the testing programme described here.

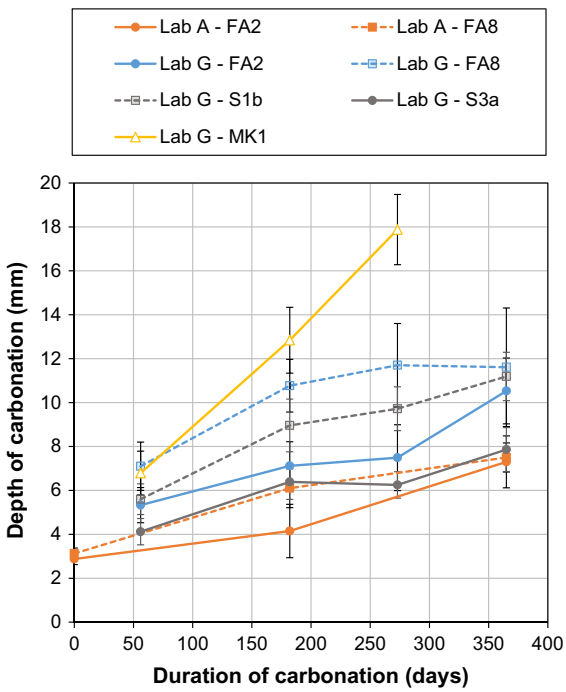


**Fig. 3** Results of carbonation testing under natural outdoor conditions protected from rainfall ('sheltered'). *Error bars* represent one standard deviation in each direction from the mean, within the results recorded by each laboratory

### 4.3 Natural carbonation testing—outdoor

Figure 3 shows the results of the natural carbonation testing conducted under outdoor natural conditions protected from rainfall (sheltered). Because of the limited number of data points, and the probability that the outdoor exposure conditions differed significantly between participating laboratories, an evaluation of the data regarding sd and COVs, as well as of the performance of fly ash-based concretes versus BFS-based concretes, seems not to be justified.

However, two key points may be noted. Firstly, as with the results described above for accelerated and indoor conditions, the relative order of the performance in terms of depths of carbonation was always in the expected order for the high-performance concretes versus the moderate-performance concretes of the same class.

Secondly, as shown in Figs. 2 and 3, the depths of carbonation of FA2 and FA8 at the start of exposure (0 days as plotted on the graphics here) were always significantly higher than 0 mm, in the cases where these were measured. This initial carbonation was observed even though the curing of the concretes was scheduled to take place for 2 days in the covered or sealed moulds and thereafter in tightly closed plastic bags. Evidently, this did not suffice to prevent initial carbonation during curing. This tendency to carbonate rapidly at early age is caused by the high alkalinity of the concrete pore solutions, and the comparatively slow microstructural evolution of fly ash-based alkali-activated concretes. An analogous observation of higher susceptibility to carbonation at early age of slower-hardening cements has been made previously in a comparison of Portland cement and blends [44]. Unfortunately, initial depths of carbonation were not measured by any laboratories for the BFS-based and the metakaolin-based concretes in the present round robin, but for the reasons outlined above it can be assumed that incipient carbonation had also occurred in these concretes before being first exposed to the carbonation environments.

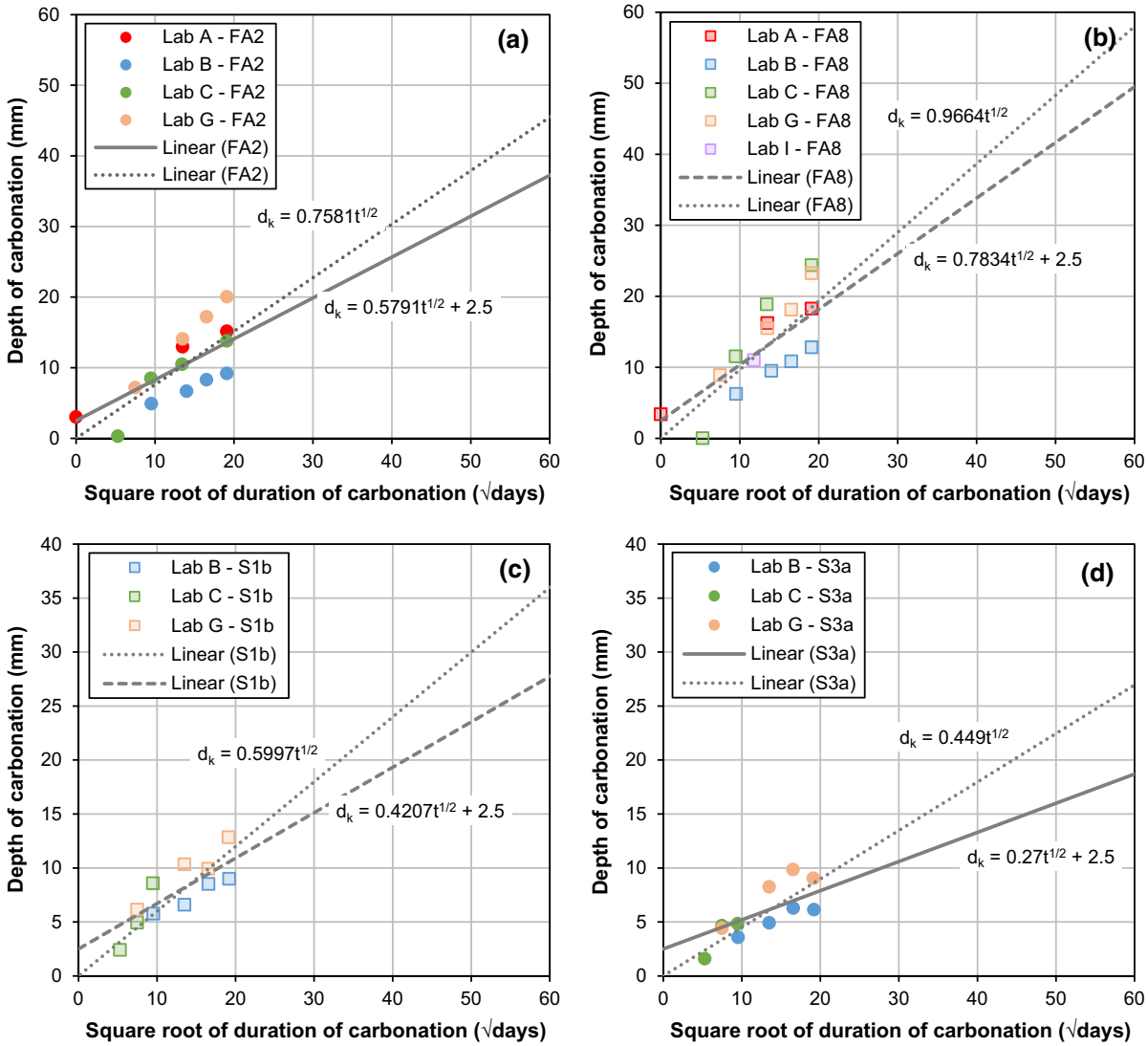


**Fig. 4** Results of carbonation testing under conditions approximating natural exposure ('indoor') of **a** the fly ash-based concrete FA2, **b** the fly ash-based concrete FA8, **c** the BFS-based concrete S1b, **d** the BFS-based concrete S3a, in each case extrapolated to 3600 days (approx. 10 years) from data gathered within the first year. Fits to the data, applying the square root-of-time law and assuming either zero initial depth of carbonation (dotted lines) or an initial depth of carbonation of 2.5 mm (dashed lines and full lines) are given to demonstrate the importance of the assumed starting condition on the outcome of extrapolations. Note the different ranges of the ordinates in panels **a** and **b** versus panels **c** and **d**

These considerations have implications for the extrapolation of data from natural carbonation testing to exposure durations longer than the maximum test duration. As an example, Fig. 4 shows the projection of depths of carbonation of the fly ash-based and BFS-based alkali-activated concretes up to 3600 days ($\sim$ 10 years), calculated by fitting to the experimental data the well-known square root-of-time law ($d_k = k' \times t^{0.5} + K_0$, where $d_k$ is the depth of carbonation, $t$ is the duration of carbonation, and $k'$ and $K_0$ are constants [45]).[3] Fitting was conducted using the mean result from each laboratory, assuming an initial depth of carbonation ($K_0$) of either 0 mm or 2.5 mm. For all

[3] The use of the square-root-of-time law in these example calculations is not meant to imply that it is generally applicable without modifications to alkali-activated concretes, but rather serves to demonstrate the influence of the chosen starting conditions on the outcomes of extrapolations.

concretes, the calculated depths at 3600 days of carbonation are ~ 8 mm higher when an initial depth of carbonation of 0 mm is assumed. This would represent a significant underestimation of the actual carbonation resistance in real-world applications, compared to the use of a non-zero estimate of the depth of carbonation.

It is also notable that the extrapolation of the carbonation data to calculate the time taken to carbonate up to realistic minimum cover depths (20–30 mm) yields values of less than 10 years for three of the four concretes studied here. This means that it is particularly important to understand the interplay between carbonation and steel corrosion in alkali-activated binders, because if the simplified transport model used here is valid over these time periods, the first reinforcing elements are likely to be surrounded by carbonated concrete well within the usual expected service life of a concrete element. There is experimental evidence to indicate that carbonated low-calcium AAM binders are actually able to remain effective in protecting mild steel from corrosion due to the high residual alkalinity of the pore fluid [38], so the results presented here do not directly indicate that carbonation will limit service life to unacceptably short values, but prudence is nonetheless justified in selecting binders for use in reinforced concrete under aggressive conditions. Mix S3a here shows good carbonation resistance, and may be attractive as an option for use in this application.

### 4.4 Chloride penetration testing

Figure 5 shows the results of the accelerated chloride penetration testing and the rapid chloride migration (RCM) testing for the five alkali-activated concretes. The concretes based on low-Ca precursors generally exhibited about two orders of magnitude higher chloride transport/migration coefficients than the BFS-based concretes. This is expected, as alkali-activated BFS concretes develop a finer pore structure [35], and in many cases are able to bind substantial amounts of $Cl^-$, particularly via adsorption onto and incorporation into AFm phases and/or hydrotalcite-like phases [15, 46].

In every laboratory where accelerated chloride penetration testing according to NT BUILD 443 was applied to multiple concrete mixes, FA2 exhibited a lower chloride transport coefficient than FA8 in a within-laboratory comparison, while S3a exhibited a higher chloride transport coefficient than S1b (Fig. 5a). Since S3a has a higher compressive strength than S1b [24] (and thus is called the 'high-performance' concrete among the pair of BFS-based materials tested here), and exhibited lower depths of carbonation than S1b in all carbonation tests, its higher chloride transport coefficients may be considered to be contrary to expectations. However, the two BFS-based concretes had different binder contents as well as different activator compositions (Table 1). These two mix-design parameters affect the pore structure and phase assemblage evolution of alkali-activated slag concretes so that a direct correlation between its influence on compressive strength, and carbonation resistance or chloride penetration resistance, is not usually identified [16, 47]. A detailed understanding of these effects in the studied concretes would require microstructural data that are presently not available for these specific concretes; nevertheless, the round robin results serve to demonstrate that compressive strength is not necessarily a good indicator of the durability performance of alkali-activated concretes when comparing mix designs.

To explore this in more detail for specific comparison between concretes of a single (notional) mix design but differing compressive strengths, Fig. 6 presents a comparison between the chloride migration coefficients ($D_{nssm}$) and the 28-day compressive strengths reported for each of the BFS-based mixes by each participating laboratory; strength data are from [24]. This illustrates clearly that there is not a direct relationship between concrete compressive strength and resistance to chloride ingress, among each set of concretes with the same binder composition and notionally the same mix design (but using local aggregates in each case). The factors influencing compressive strength within this round robin testing programme were explored in detail in [24].

The chloride migration coefficients obtained through application of the RCM test were generally in reasonable agreement with the transport coefficients obtained by accelerated chloride penetration (ponding) testing. However, the ranking of the high-performance concretes versus the moderate-performance concretes in each type of concrete was not consistently repeated in the RCM tests. For example, a higher migration coefficient was obtained for FA2 than for FA8 in laboratory *C*, and a lower migration

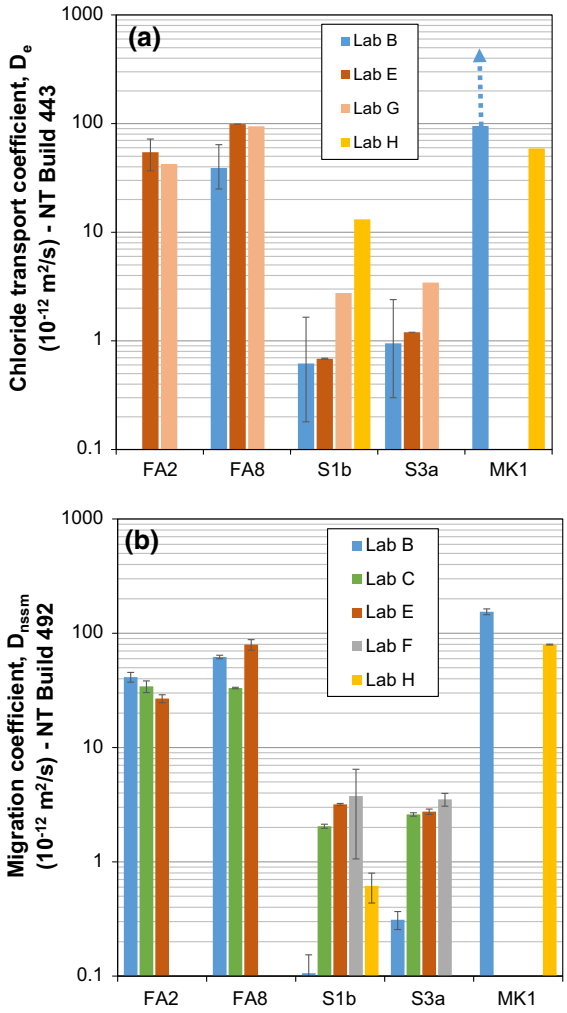


**Fig. 5** Results of **a** accelerated chloride penetration testing according to NT BUILD 443, **b** rapid chloride migration (RCM) testing according to NT BUILD 492. Accelerated chloride penetration testing results were obtained by a modified method in laboratory *B*, see Sect. 2.4. The *arrow* in panel **a** indicates that the displayed value is a lower bound on the actual $D_e$ value. *Error bars* represent one standard deviation in each direction from the mean, or estimated errors for NT BUILD 443 in laboratory *B*

coefficient was obtained for S3a than for S1b in laboratories *E* and *F* (Fig. 5b). There are various possible reasons for these inconsistencies of the RCM test results. A higher variability could be caused by difficulties in taking readings from the BFS-based concretes after testing and spraying $AgNO_3$, because the chloride penetration depths are usually on the order of a few millimetres, i.e. generally less than the maximum aggregate size of the concretes. In addition,

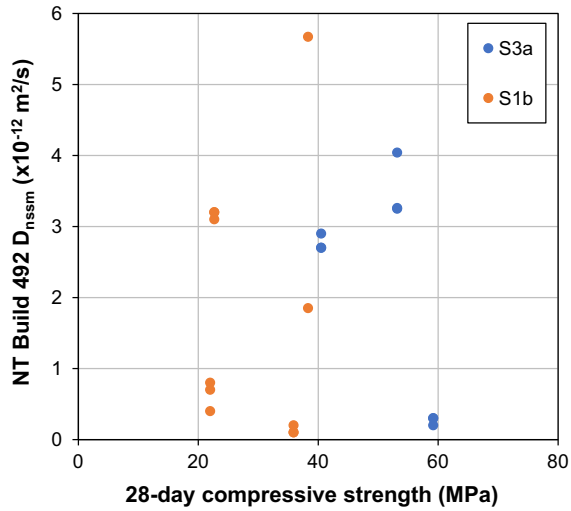


**Fig. 6** Correlation between $D_{nssm}$ values determined according to NordTest NT Build 492 by each laboratory (showing individual data points for replicate tests), and the mean 28-day compressive strength measured in the same laboratory, for concretes S3a and S1b

differences in the pH of the pore solution will cause the $Cl^-$ concentration at the colour change boundary to deviate from 0.07 M [11], which is the value assumed for the computation of the migration coefficients according to NT BUILD 492 [31]. There are indications that the assumption of a $Cl^-$ concentration of 0.07 M at the colour change boundary seems not to hold even for Portland cements and Portland cement-BFS blends. Specifically, Maes et al. [48] have determined $AgNO_3$ colour change values in the range 0.13–0.45 M $Cl^-$ for concretes based on those binders, meaning that future work in understanding and defining colour change boundaries in $AgNO_3$ spraying, extending the existing literature e.g. [31, 49], would certainly be valuable in understanding the testing of alkali-activated concretes.

A comparison between the results obtained according to NT BUILD 443 and NT BUILD 492 is shown in Fig. 7 for the cases where both tests have been performed on the same concrete mix-design in a laboratory. The limited data do not allow clear conclusions to be drawn about the possible existence or absence of any systematic bias between the two methods in the testing of alkali-activated concretes.

Figure 8 shows the results of the rapid chloride permeability testing (RCPT); only the BFS-based AAM concretes provided useable data, as the others

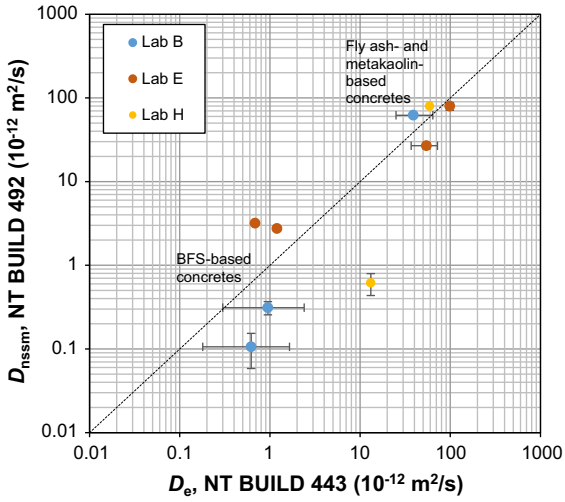


**Fig. 7** Comparison of chloride transport/migration coefficients obtained according to NT BUILD 443 and NT BUILD 492. The line of equality is given as a dashed line. *Error bars* represent one standard deviation in each direction from the mean, or estimated errors for NT BUILD 443 in laboratory B

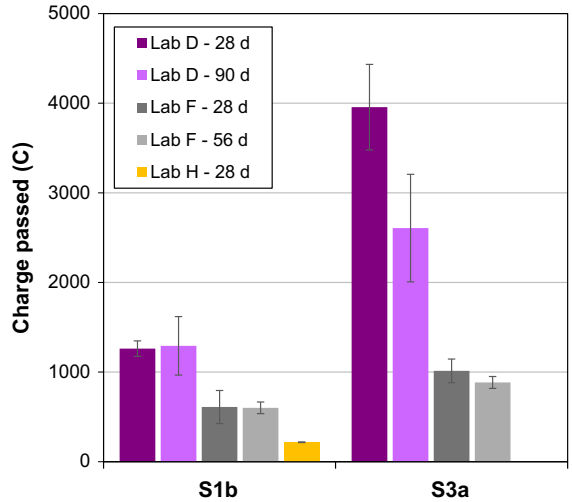


**Fig. 8** Results of rapid chloride permeability testing (RCPT) according to ASTM C1202 [32], for the BFS-based AAM concretes at curing ages as identified in the legend. *Error bars* represent one standard deviation in each direction from the mean, for the results within each laboratory

led to overheating of the test apparatus due to the high conductivity of the test specimens under the application of a high voltage. The RCPT method has been criticised in the past because its outcomes depend substantially on the composition of the pore solution of the test specimen, rather than being defined by its pore structure and actual chloride penetration resistance [50, 51]. Furthermore, ASTM C1202 [32] explicitly states that its applicability is limited to types of concrete where correlations between conductivity and chloride ponding tests have been established, and this is not yet the case for alkali-activated concretes. In the present round robin, the relative order of the results obtained in each laboratory for the two BFS-based concretes was consistent with the ranking from the NordTest NT BUILD 443 ponding test. However, the large inter-laboratory deviations (up to 5.8 × variability for corresponding concretes), and the fact that the pore refinement expected at longer curing times [35] is not always reflected in the results in Fig. 8, suggest that the standardised RCPT method may have limited applicability to AAMs. This may be related to the effect of the pore solution composition and/or other factors. Testing under a reduced voltage has been proposed as a means of mitigating this problem [52], and is under investigation in the ongoing work programme of RILEM TC 283-CAM.

For all three methods employed to determine chloride penetration resistance (NT BUILD 443, NT BUILD 492, ASTM C1202), the COVs computed from the mean results reported by the different laboratories were in the range 17.5–43.1% for the fly ash-based concretes, and 60.2–89.9% for the BFS-based concretes, with no apparent systematic difference between the methods (Tables S11–S13).[4] For comparison, NT BUILD 443 [27] states an expected COV of 15% for the chloride transport coefficient; NT BUILD 492 [29] reports a 9% COV of repeatability in the non-steady-state migration coefficient from a six-laboratory round robin; and ASTM C1202 [32] gives the multilaboratory COV of a single test result as 18.0%. In previously reported round robins on Portland and blended cement-concretes [53, 54] the following reproducibility COVs were found: 16–53% for the NT BUILD 443 chloride transport coefficient; 12–37% for the NT BUILD 492 non-steady-state migration coefficient; and 16–24% for the ASTM C1202 charge passed. Aït-Mokhtar et al. [34] determined COVs of 12.4–25.4% for non-steady-state migration coefficients of different batches of three

[4] For the calculation of the COV for the accelerated chloride penetration testing, the result of laboratory *H* for concrete S1b was excluded because it was identified as an outlier (confidence > 90%) by the *Q* test.

different blended cement-concretes by a method similar to NT BUILD 492, which gives an indication of the typical variability of concrete properties.

The COVs obtained in the present round robin include any variations of the concrete properties caused by production in different laboratories and use of different aggregates, as well as any between-laboratory variability of the test methods. Considering this, the COVs appear to indicate that the precision of the methods described in NT BUILD 443 and NT BUILD 492 is of the same order for the fly ash-based alkali-activated concretes as for conventional (Portland or blended cement-based) concretes. However, the inability of the RCM test (NT BUILD 492) to consistently reproduce the relative ranking of high-performance versus moderate-performance concretes, that was observed in accelerated chloride penetration testing (NT BUILD 443) (Fig. 5), may indicate that the latter method is more reliable than the RCM test, or alternatively may indicate that the expected rankings based on strength are not consistent with the real performance of the materials (at least under an applied electric potential). The COVs of the mean results obtained by these two methods were considerably larger for the BFS-based concretes than for the fly ash-based concretes. It is tempting to attribute this observation to the much lower transport coefficients of the BFS-based materials; e.g., for the readings taken after spraying $AgNO_3$ solution in the RCM test, the low penetration depths may be a cause for larger scatter, as discussed above. As for the NT BUILD 443 method, laboratories tended to obtain less layers in profile grinding, and thus less chloride profile data points, for samples with a lower penetration depth, which may cause lower reliability of the curve-fitting procedure for the former; however, this relationship remains to be proven.

Finally, it is noted that all three methods employed to determine the chloride penetration resistance involve storage of the concrete samples either in saturated $Ca(OH)_2$ solution (NT BUILD 443 and NT BUILD 492) or soaking in water (ASTM C1202). This inevitably leads to leaching of sodium ions from the concrete specimens and, in the case of storage in $Ca(OH)_2$ solution, to diffusion of calcium ions into the concrete specimens, changing the composition of the pore solution composition at least in the outer regions of the samples. However, the extent to which this occurs and its impact on the results of the testing methods has not been assessed in the present round robin. It is possible that pre-conditioning of alkali-activated concretes in a solution more representative of their pore solution chemistry (e.g. NaOH at concentrations of 0.5–2.0 mol/L depending on the mix design) could give more consistent and representative results, but the present study did not extend to confirmation of this hypothesis.

## 5 Conclusions

Accelerated carbonation testing in an atmosphere with a $CO_2$ concentration of 1% (EN 13295) appears to be suitable to correctly rank different alkali-activated concretes with the same type of binder chemistry, in an acceptably short time. However, a more realistic assessment of the performance of alkali-activated concretes under in-service conditions, including differentiation of alkali-activated concretes with different binders, can only be obtained by testing using natural levels of $CO_2$. Extrapolation of test results to predict future depths of carbonation should consider carbonation that occurs during initial curing, even under curing conditions designed to limit access of air to the concrete specimens. Further studies are required to assess to what extent results obtained at constant RH in the range 50–65% deviate from performance under natural outdoor exposure conditions, in which the RH is changing and can approach much higher values.

Rapid chloride migration testing (NT BUILD 492) allows different classes of alkali-activated concretes to be differentiated, but does not consistently rank alkali-activated concretes according to expected performance levels, even when they have the same type of binder. Conversely, accelerated chloride penetration testing by ponding (NT BUILD 443) appears to give reliable results for different alkali-activated concretes, although at the cost of a greatly extended test duration. Nevertheless, the usually high chloride transport resistances of BFS-based concretes cause a comparatively low precision of both methods when applied to these concretes. Thus, further improvements of both methods appear to be desirable when they are to be applied to concretes of low permeability.

The limited data obtained with the rapid chloride permeability test (ASTM C1202) on alkali-activated BFS concretes were broadly in line with the results of the NT BUILD 443 method, indicating that at least a

qualitative assessment of the chloride penetration resistance of these concretes is possible with the rapid chloride permeability test. However, the inter-laboratory variation in results was very high, and testing of other classes of alkali-activated concretes by this method was not successful; thus, it remains to be clarified whether the method can be applied to alkali-activated concretes based on binders other than BFS. It is likely that modification of this method would be needed, based on the technical challenges associated with its direct application, if meaningful results are to be gained for AAM concretes, and this is the subject of ongoing work within RILEM Technical Committee 283-CAM as a successor to TC 247-DTA.

## 6 Compliance with ethical standards

The participation of J. L. Provis and S. A. Bernal in this research was sponsored by the Engineering and Physical Sciences Research Council (EPSRC; UK) under grant number EP/M003272/1. The participation of A. Castel in this research was funded by the Cooperative Research Centre (CRC) for Low Carbon Living Ltd supported by the Cooperative Research Centres, an Australian Government initiative. Participation of V. Ducman was financially supported by the Slovenian Research Agency Programme Group P2-0273. The work and research of K. Dombrowski-Daube in RILEM TC-247 DTA was supported by ZIM—Central Innovation Program, German Federal Ministry of Economic Affairs and Energy (BMWi) by order of the German Bundestag. The contribution of the team at TU Delft led by G. Ye was supported by the Materials innovation institute M2i/Netherlands Organisation for Scientific Research (STW/M2i project 13361). The contributions of K. Arbi were also supported by Delta Concrete Consult BV.

**Acknowledgements** The authors would like to thank all members of RILEM TC 247-DTA for the valuable discussions in planning the activities for the round robin. Particularly we would like to acknowledge the immense contribution of A. Buchwald (ASCEM, Netherlands), W. Rickard and A. van Riessen (Curtin University, Australia), G. Gluth (BAM, Germany), R. Pouhet and M. Cyr (Toulouse University, France) in developing the concrete mix designs evaluated; and for arranging the donations of raw materials, and the logistics for their distribution to all the round robin participants. The participation of Dr Andrew Dunster (BRE, United Kingdom) in the round-robin testing and enriching the associated discussions is very gratefully acknowledged. We greatly appreciate the help of colleagues, laboratory assistants and students in the participating laboratories, including Rajetharan Krishnakumar, Zhijun Tan, Maria Criado and Oday Hussein at the University of Sheffield. Special thanks are also due to Ecocem (France), BauMineral (Germany) and Argeco (France) for the generous donation of several tonnes of slag, fly ash and flash-calcined metakaolin to the members of this technical committee; and to PQ Corporation and Grupo IQE for the donation of activator constituents to some of the participating laboratories.

**Compliance with ethical standards**

**Conflict of interest** The authors declare no competing financial interests.



## References

1. Provis JL, van Deventer JSJ (2014) Alkali-activated materials: state-of-the-art report, RILEM TC 224-AAM. Springer, Dordrecht
2. Xu H, Provis JL, van Deventer JSJ, Krivenko PV (2008) Characterization of aged slag concretes. ACI Mater J 105(2):131–139
3. Buchwald A, Vanooteghem M, Gruyaert E, Hilbig H, Belie N (2015) Purdocement: application of alkali-activated slag cement in Belgium in the 1950s. Mater Struct 48(1–2):501–511
4. Bernal SA, Provis JL (2014) Durability of alkali-activated materials: progress and perspectives. J Am Ceram Soc 97(4):997–1008
5. Bernal SA, Provis JL, Walkley B, San Nicolas R, Gehman JD, Brice DG, Kilcullen AR, Duxson P, van Deventer JSJ (2013) Gel nanostructure in alkali-activated binders based on slag and fly ash, and effects of accelerated carbonation. Cem Concr Res 53:127–144
6. Glasser FP, Marchand J, Samson E (2008) Durability of concrete—degradation phenomena involving detrimental chemical reactions. Cem Concr Res 38(2):226–246
7. Galan I, Glasser FP (2015) Chloride in cement. Adv Cem Res 27:63–97

8. Criado M (2015) The corrosion behaviour of reinforced steel embedded in alkali-activated mortar. In: Pacheco-Torgal F, Labrincha JA, Leonelli C, Palomo A, Chindaprasirt P (eds) Handbook of alkali-activated cements, mortars and concretes. Woodhead, Cambridge, pp 333–372
9. Mundra S, Bernal SA, Criado M, Hlaváček P, Ebell G, Reinemann S, Gluth GJG, Provis JL (2017) Steel corrosion in reinforced alkali-activated materials. RILEM Tech Lett 2:33–39
10. Law D, Adam A, Molyneaux T, Patnaikuni I (2012) Durability assessment of alkali activated slag (AAS) concrete. Mater Struct 45(9):1425–1437
11. Ismail I, Bernal SA, Provis JL, San Nicolas R, Brice DG, Kilcullen AR, Hamdan S, van Deventer JSJ (2013) Influence of fly ash on the water and chloride permeability of alkali-activated slag mortars and concretes. Constr Build Mater 48:1187–1201
12. Bernal SA, San Nicolas R, Provis JL, Mejía de Gutiérrez R, van Deventer JSJ (2014) Natural carbonation of aged alkali-activated slag concretes. Mater Struct 47(4):693–707
13. Ma Q, Nanukuttan SV, Basheer PAM, Bai Y, Yang C (2016) Chloride transport and the resulting corrosion of steel bars in alkali activated slag concretes. Mater Struct 49:3663–3677
14. Gunasekera C, Law DW, Setunge S (2016) Long term permeation properties of different fly ash geopolymer concretes. Constr Build Mater 124:352–362
15. Ke X, Bernal SA, Hussein OH, Provis JL (2017) Chloride binding and mobility in sodium carbonate-activated slag pastes and mortars. Mater Struct 50(6):252
16. Babaee M, Castel A (2018) Chloride diffusivity, chloride threshold, and corrosion initiation in reinforced alkali-activated mortars: role of calcium, alkali, and silicate content. Cem Concr Res 111:56–71
17. Babaee M, Castel A (2016) Chloride-induced corrosion of reinforcement in low-calcium fly ash-based geopolymer concrete. Cem Concr Res 88:96–107
18. Tennakoon C, Shayan A, Sanjayan JG, Xu A (2017) Chloride ingress and steel corrosion in geopolymer concrete based on long term tests. Mater Des 116:287–299
19. Häkkinen T (1987) Durability of alkali-activated slag concrete. Nord Concr Res 6(1):81–94
20. Krivenko PV (1999) Alkaline cements: structure, properties, aspects of durability. In: Krivenko PV (ed) Proceedings of the second international conference on alkaline cements and concretes. Kiev, Ukraine, Oranta, pp 3–43
21. Douglas E, Bilodeau A, Malhotra VM (1992) Properties and durability of alkali-activated slag concrete. ACI Mater J 89(5):509–516
22. Al-Otaibi S (2008) Durability of concrete incorporating GGBS activated by water-glass. Constr Build Mater 22(10):2059–2067
23. Bondar D, Ma Q, Soutsos M, Basheer M, Provis JL, Nanukuttan S (2018) Alkali activated slag concretes designed for a desired slump, strength and chloride diffusivity. Constr Build Mater 190:191–199
24. Provis JL, Arbi K, Bernal SA, Bondar D, Buchwald A, Castel A, Chithiraputhiran S, Cyr M, Dehghan A, Dombrowski-Daube K, Dubey A, Ducman V, Dunster A, Gluth GJG, Nanukuttan S, Peterson K, Puertas F, van Riessen A, Torres-Carrasco M, Ye G, Zuo Y (2019) RILEM TC 247-DTA round robin test: mix design and reproducibility of compressive strength of alkali-activated concretes. Mater Struct 52:99
25. European Committee for Standardization (CEN) (2004) Products and systems for the protection and repair of concrete structures—test methods—determination of resistance to carbonation (EN 13295:2004), Brussels, Belgium
26. European Committee for Standardization (CEN) (2007) Testing hardened concrete—part 10: determination of the relative carbonation resistance of concrete (DD CEN/TS 12390-10: 2007), Brussels, Belgium
27. NordTest (1995) Concrete, hardened: accelerated chloride penetration (NT BUILD 443). Espoo, Finland
28. Tang L, Gulikers J (2007) On the mathematics of time-dependent apparent chloride diffusion coefficient in concrete. Cem Concr Res 37:589–595
29. Build NT (1999) 492. Concrete mortar and cement-based repair materials: chloride migration coefficient from non-steady state migration experiments. Espoo, Finland
30. Tang L, Nilsson L-O (1992) Rapid determination of the chloride diffusivity in concrete by applying an electrical field. ACI Mater J 89(1):49–53
31. Yuan Q, Shi C, He F, De Schutter G, Audenaert K, Zheng K (2008) Effect of hydroxyl ions on chloride penetration depth measurement using the colorimetric method. Cem Concr Res 38(10):1177–1180
32. ASTM International (2012) Standard test method for electrical indication of concrete's ability to resist chloride ion penetration (ASTM C1202–12). West Conshohocken, PA
33. Gluth GJG, Rickard W (2015) Design and characterization of fly ash-based geopolymer concretes for a round-robin durability testing program. In: Leonelli C, Romagnoli M (eds) Geopolymers: the route to eliminate waste and emissions in ceramic and cement manufacturing. Engineering Conferences International/Società Ceramica Italia, Hernstein, pp 67–70
34. Aït-Mokhtar A, Belarbi R, Benboudjema F, Burlion N, Capra B, Carcassès M, Colliat JB, Cussigh F, Deby F, Jacquemot F, de Larrard T, Lataste JF, Le Bescop P, Pierre M, Poyet S, Rougeau P, Rougelot T, Sellier A, Séménadisse J, Torrenti JM, Trabelsi A, Turcry P, Yanez-Godoy H (2013) Experimental investigation of the variability of concrete durability properties. Cem Concr Res 45:21–36
35. Provis JL, Myers RJ, White CE, Rose V, van Deventer JSJ (2012) X-ray microtomography shows pore structure and tortuosity in alkali-activated binders. Cem Concr Res 42(6):855–864
36. Bernal SA, Provis JL, Brice DG, Kilcullen AR, Duxson P, van Deventer JSJ (2012) Accelerated carbonation testing of alkali-activated binders significantly underestimates service life: the role of pore solution chemistry. Cem Concr Res 42(10):1317–1326
37. Pouhet R, Cyr M (2016) Carbonation in the pore solution of metakaolin-based geopolymer. Cem Concr Res 88:227–235
38. Babaee M, Khan MSH, Castel A (2018) Passivity of embedded reinforcement in carbonated low-calcium fly ash-based geopolymer concrete. Cem Concr Compos 85:32–43
39. Eugster HP (1966) Sodium carbonate-bicarbonate minerals as indicators of $P_{CO2}$. J Geophys Res 71(14):3369–3377

40. Leemann A, Moro F (2017) Carbonation of concrete: the role of $CO_2$ concentration, relative humidity and $CO_2$ buffer capacity. Mater Struct 50(1):30
41. Leemann A, Nygaard P, Kaufmann J, Loser R (2015) Relation between carbonation resistance, mix design and exposure of mortar and concrete. Cem Concr Compos 62:33–43
42. Harrison TA, Jones MR, Newlands MD, Kandasami S, Khanna G (2012) Experience of using the prTS 12390-12 accelerated carbonation test to assess the relative performance of concrete. Mag Concr Res 64(8):737–747
43. Jones MR, Dhir RK, Newlands MD, Abbas AMO (2000) A study of the CEN test method for measurement of the carbonation depth of hardened concrete. Mater Struct 33(2):135–142
44. Herterich JA, Black L, Richardson IG (2015) Microstructure and phase assemblage of low-clinker cements during early stages of carbonation. In: 14th International Congress on the Chemistry of Cement. Beijing, China, China Building Materials Academy. CD-ROM proceedings
45. Page CL, Treadaway KWJ (1982) Aspects of the electrochemistry of steel in concrete. Nature 297(5862):109–115
46. Ke X, Bernal SA, Provis JL (2017) Uptake of chloride and carbonate by Mg-Al and Ca-Al layered double hydroxides in simulated pore solutions of alkali-activated slag cement. Cem Concr Res 100:1–13
47. Bernal SA, Mejía de Gutierrez R, Pedraza AL, Provis JL, Rodríguez ED, Delvasto S (2011) Effect of binder content on the performance of alkali-activated slag concretes. Cem Concr Res 41(1):1–8
48. Maes M, Gruyaert E, De Belie N (2013) Resistance of concrete with blast-furnace slag against chlorides, investigated by comparing chloride profiles after migration and diffusion. Mater Struct 46(1):89–103
49. He F, Shi C, Yuan Q, Chen C, Zheng K (2012) $AgNO_3$-based colorimetric methods for measurement of chloride penetration in concrete. Constr Build Mater 26(1):1–8
50. Shi CJ (2004) Effect of mixing proportions of concrete on its electrical conductivity and the rapid chloride permeability test (ASTM C1202 or ASSHTO T277) results. Cem Concr Res 34(3):537–545
51. Olsson N, Lothenbach B, Baroghel-Bouny V, Nilsson L-O (2018) Unsaturated ion diffusion in cementitious materials – The effect of slag and silica fume. Cem Concr Res 108:31–37
52. Noushini A, Castel A (2018) Performance-based criteria to assess the suitability of geopolymer concrete in marine environments using modified ASTM C1202 and ASTM C1556 methods. Mater Struct 51(6):146
53. Castellote M, Andrade C (2006) Round-Robin Test on methods for determining chloride transport parameters in concrete. Mater Struct 39(10):955
54. Tang L, Sørensen HE (2001) Precision of the Nordic test methods for measuring the chloride diffusion/migration coefficients of concrete. Mater Struct 34(8):479